Materials Today Physics 33 (2023) 101034

Contents lists available at ScienceDirect

Materials Today Physics

journal homepage: www.journals.elsevier.com/materials-today-physics

High-performance fully transparent Ga_2O_3 solar-blind UV photodetector with the embedded indium–tin–oxide electrodes

Chao Zhang [a,b], Kewei Liu [a,b,*], Qiu Ai [a], Xuan Sun [a,b], Xing Chen [a,b], Jialin Yang [a], Yongxue Zhu [a], Zhen Cheng [a], Binghui Li [a], Lei Liu [a,b], Dezhen Shen [a,b,**]

[a] State Key Laboratory of Luminescence and Applications, Changchun Institute of Optics, Fine Mechanics and Physics, Chinese Academy of Sciences, Changchun, 130033, China

[b] Center of Materials Science and Optoelectronics Engineering, University of Chinese Academy of Sciences, Beijing, 100049, China

ARTICLE INFO

Keywords:
Solar-blind UV detector
Ga_2O_3 film
Transparent
Indium–tin–oxide
Embedded electrodes

ABSTRACT

Transparent ultraviolet (UV) photodetectors have attracted the increasing attention due to their giant potential in integrated transparent electronics applications. In this work, a fully transparent metal-semiconductor-metal (MSM) solar-blind UV photodetector with embedded indium–tin–oxide (ITO) electrodes based on Ga_2O_3 films was successfully designed and constructed for the first time. A novel method to prepare a MSM photodetector with embedded electrode structure is proposed by selective epitaxying β-Ga_2O_3 thin films on *c*-plane sapphire substrate with ITO inter-digital electrodes prepared in advance. An ultra-low dark current of 1.6 pA, a superb UV-to-visible rejection ratio of 1.3×10^6 (R_{250}/R_{400}), a high specific detectivity of 7.4×10^{15} Jones and a large responsivity of 74.9 A/W can be observed in our device at 10 V, which are superior to those of other reported transparent UV photodetectors based on Ga_2O_3 films. The strong and uniform electrical field in β-Ga_2O_3 between two adjacent embedded ITO electrodes, and the high quality of β-Ga_2O_3 films should be responsible the excellent solar-blind photodetection performance. Our findings pave a new way to realize a high-performance fully transparent Ga_2O_3 solar-blind UV photodetector, which has the giant potential for applications in future transparent electronics.

1. Introduction

Solar-blind ultraviolet (UV) photodetectors show numerous applications in various fields, including missile warning, environment monitoring, space research, flame detection, and so on [1–5]. Wide bandgap semiconductor materials, such as diamond, ZnMgO, AlGaN and Ga_2O_3, have great potential for application in the UV photodetectors for their unique physical and chemical properties [6–11]. As the emerging wide bandgap semiconductor material, Ga_2O_3 is considered as an ideal material for the solar-blind photodetection, which benefits from its very suitable bandgap (4.7–5.3 eV), excellent chemical inertness, thermal stability and high radiation hardness [12–15]. To date, a large number of Ga_2O_3-based photodetectors with different structural types have been demonstrated, including metal−semiconductor−metal (MSM) structure, Schottky junction and heterojunction [16–19]. Among them, owing to the fast response speed, simple fabrication process and easy integration with other devices, the inter-digitated MSM structure has become the most common architecture of Ga_2O_3 solar-blind UV photodetectors [14,20]. It is not uncommon to achieve large responsivity (>100 A/W) [21], high UV-to-Visible rejection ratio (>10^5) [22], and high specific detectivity (>10^{14} Jones) [23] in Ga_2O_3 MSM photodetectors. Recently, transparent electronics, as an promising technology for next generation electronic and optoelectronic devices, have attracted increasing attention in various applications [24–27]. In particular, transparent UV photodetectors are crucial for integrated transparent electronics applications, such as some smart windows, transparent display panels, transparent batteries, and so on [28–30]. However, for the most reported Ga_2O_3 MSM photodetectors, the opaque metals with high electrical conductivity have been employed as electrodes materials, which hinder applications of the devices in transparent electronics.

* Corresponding author. State Key Laboratory of Luminescence and Applications, Changchun Institute of Optics, Fine Mechanics and Physics, Chinese Academy of Sciences, Changchun, 130033, China.

** Corresponding author. State Key Laboratory of Luminescence and Applications, Changchun Institute of Optics, Fine Mechanics and Physics, Chinese Academy of Sciences, Changchun, 130033, China.

E-mail addresses: liukw@ciomp.ac.cn (K. Liu), shendz@ciomp.ac.cn (D. Shen).

https://doi.org/10.1016/j.mtphys.2023.101034
Received 13 February 2023; Received in revised form 26 February 2023; Accepted 1 March 2023
Available online 3 March 2023

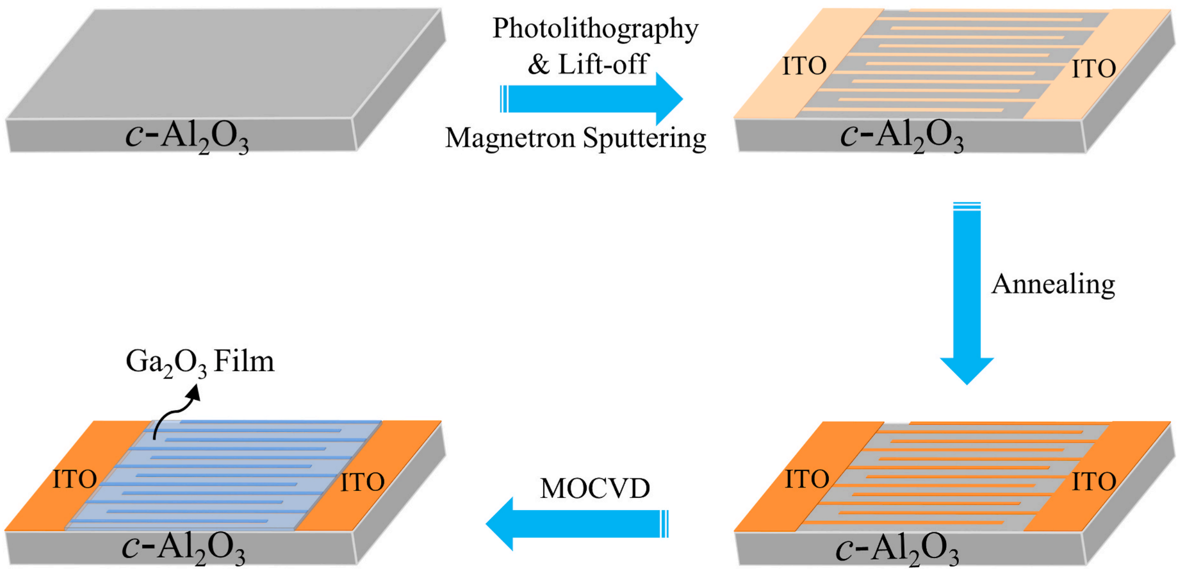

Fig. 1. Schematic diagram of fabrication processes of transparent Ga_2O_3 MSM photodetector.

Therefore, to meet the requirements of fully transparency, it is the best choice to replace the traditional metal electrodes with transparent electrodes in the UV photodetectors. So far, few reports on MSM-type Ga_2O_3 photodetectors with transparent electrodes are available [21, 31–33]. Kumar et al. reported an completely transparent and flexible amorphous Ga_2O_3 solar-blind UV device using amorphous indium-zinc-oxide (*a*-IZO) electrodes. The photodetector shows higher external quantum efficiency and responsivity compared to the device based on traditional Ag metal electrodes [31]. S. Oh et al. made the β-Ga_2O_3 film-based solar-blind photodetector using transparent graphene electrodes. In contrast to the device using Ni/Au metal electrodes, the transparent device exhibits higher performance, which is related to the absence of shading and more carriers density with the graphene electrodes [32]. However, all the reported transparent Ga_2O_3 solar-blind UV photodetectors are fabricated by conventional planar electrode structures, whose inhomogeneous electric field within the active layer is detrimental to separation or collection of photogenerated electron-hole pairs [34,35].

In our work, Ga_2O_3 films were grown using metal−organic chemical vapor deposition (MOCVD) technology on *c*-Al_2O_3 substrates with interdigital indium tin oxide (ITO) electrodes prepared in advance, and a Ga_2O_3 MSM solar-blind UV photodetector with embedded electrodes was thus fabricated for the first time. The device shows a high transmittance (over 85% in 400–700 nm range), suggesting its fully

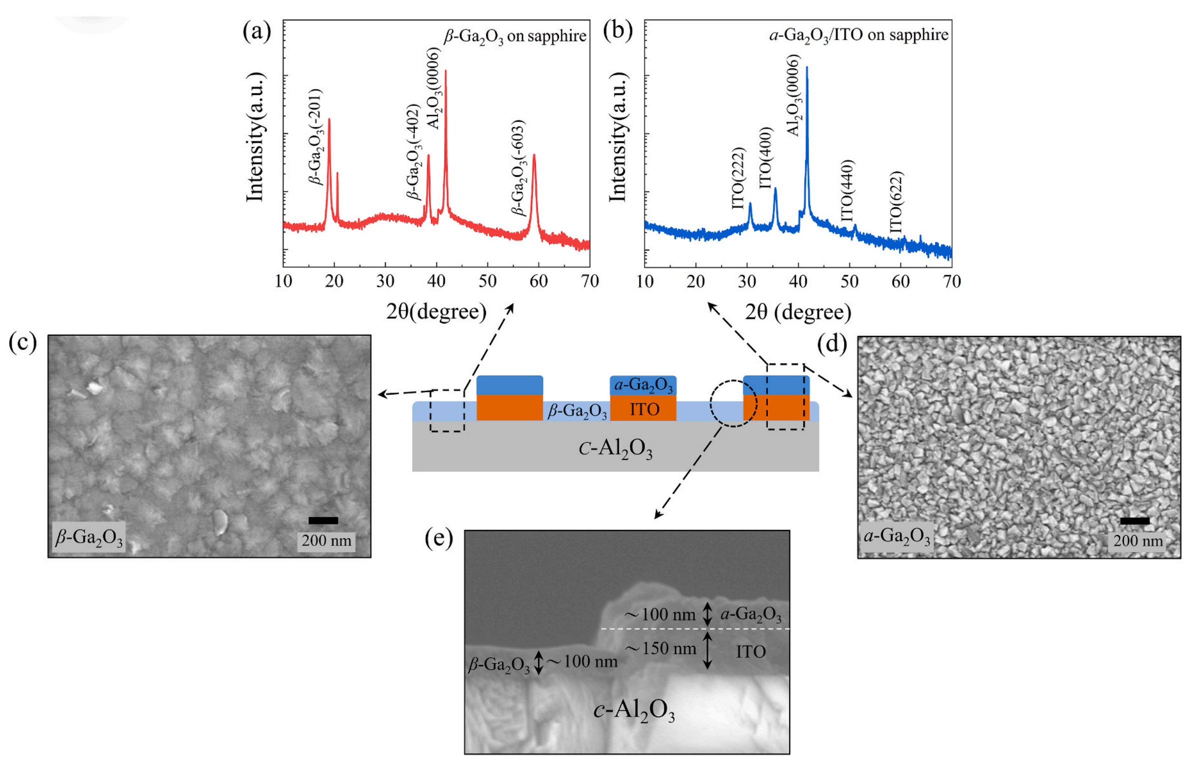

Fig. 2. XRD patterns of epitaxial Ga_2O_3 films (a) on *c*-Al_2O_3 substrate and (b) on ITO substrate. The top-view SEM images of Ga_2O_3 films (c) on *c*-Al_2O_3 substrate and (d) on ITO substrate. (e) The cross-sectional SEM image of device.

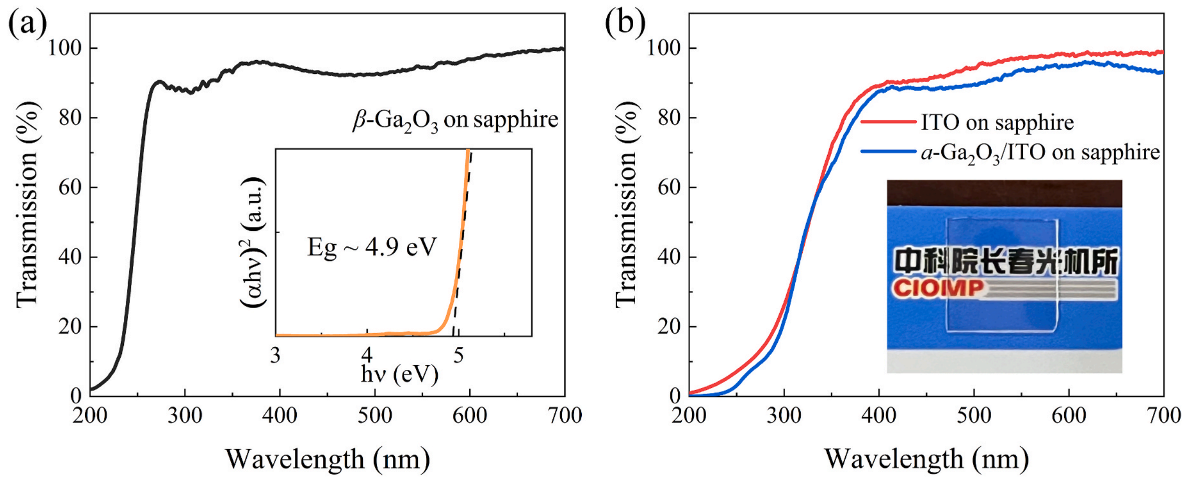

Fig. 3. Optical transmission spectra of (a) β-Ga_2O_3, (b) ITO and a-Ga_2O_3/ITO films. The inset in (a) is the Tauc's plots of film and the inset in (b) is original photograph of the device.

transparent nature. This transparent photodetector exhibits excellent solar-blind UV photodetection performance with an ultra-low dark current of 1.6 pA, a superb UV-to-visible rejection ratio of 1.3×10^6 (R_{250}/R_{400}), a large responsivity of 74.9 A/W and a high specific detectivity of 7.4×10^{15} Jones under 10 V bias. Moreover, the device also exhibits good stability and reproducibility with the quick response speed. The superb performance of our device with embedded electrodes can be attributed to more homogeneous electric field in Ga_2O_3 film, resulting in the enhancement for the separation and collection of photogenerated carriers. Our fully transparent Ga_2O_3-based MSM solar-blind UV photodetector has great application potential in integrated transparent electronics.

2. Experimental details

The schematic diagram of the fabrication processes of transparent Ga_2O_3 MSM photodetector was shown in Fig. 1. The ITO films was firstly deposited on c-plane sapphire substrate using magnetron sputtering with mixed gas flow rates of Ar (20 sccm) and O_2 (5 sccm) using the gas flow meters (pressure: ~1.3 Pa; power: 100 W). Subsequently, 25 pairs of ITO interdigital electrodes can be fabricated on sapphire by the photolithography & lift-off technique with ~500 μm long, ~10 μm wide and ~10 μm spacing. Then ITO interdigital electrodes were annealed at 750 °C under the oxygen atmosphere for 40 min to obtain a low resistance (~1.54×10^{-3} Ω cm of resistivity). After that, Ga_2O_3 films were grown on c-Al_2O_3 substrate with ITO interdigital electrodes by MOCVD, which were grown under the temperature of 700 °C with chamber pressure of 9.8×10^2 Pa. The gallium and oxygen precursors were Triethylgallium and high-purity oxygen with the flow rates of 4 and 500 sccm, respectively. Finally, transparent Ga_2O_3 MSM photodetector with embedded electrodes was demonstrated. The whole preparation process of our device does not require etching of Ga_2O_3, which not only simplifies the process, but also avoids the damage caused by etching.

The surface & cross-sectional morphologies of the films in our work were systematically characterized using scanning electron microscopy (SEM) (Hitachi S-4800) and crystalline structural properties of films were characterized using X-ray diffractometer (XRD) (Bruker D8GADDS). Transmission spectra were studied by the spectrophotometer (Shimadzu UV3101PC). For characterization of the current–voltage (I–V) and time-dependent current (I–t) were obtained using the semiconductor device analyzer (Agilent B1500A) at room temperature. The spectral response properties were measured using the UV-enhanced Xe lamp (200 W) with a monochromator.

3. Results and discussion

Fig. 2a exhibits XRD pattern of Ga_2O_3 film on c-Al_2O_3 substrate between ITO electrodes. Besides the diffraction peak from c-Al_2O_3, three peaks located at 18.88°, 38.26°, and 58.96° can be attributed to the planes (−201), (−402) and (−603) of β-Ga_2O_3, respectively (JCPDS:43–1012). In contrast, for the Ga_2O_3 film on ITO, only the diffraction peaks of ITO and sapphire were observed, indicating that the Ga_2O_3 films grown on the ITO electrodes are amorphous as shown in Fig. 2b.

Additionally, top-view SEM images of β-Ga_2O_3 films on sapphire and amorphous Ga_2O_3 (a-Ga_2O_3) films on ITO are presented in Fig. 2c and d, respectively. Clearly, both two films have smooth surface and the grain size of β-Ga_2O_3 film is much larger than that of a-Ga_2O_3 film. At the same

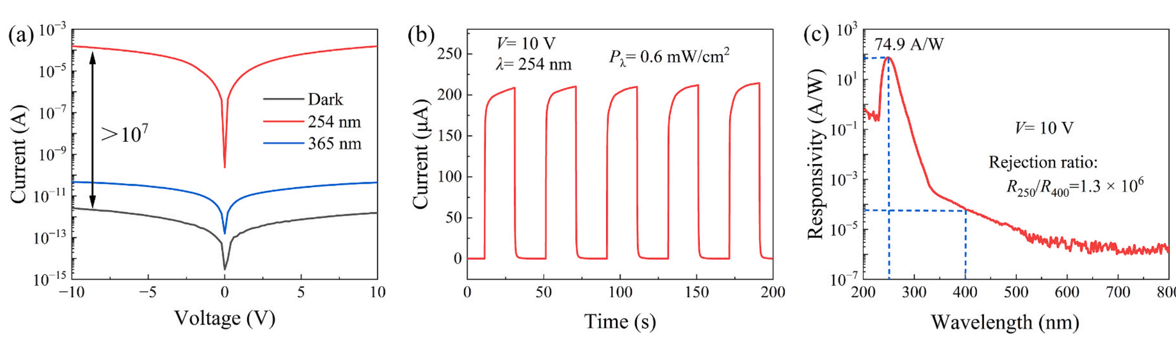

Fig. 4. (a) Semilogarithmic I–V characteristic curves of the device in dark and under UV light (254 and 365 nm). (b) I-t photoresponse curve with 254 nm illumination under 10 V bias. (c) Spectral response of the device under 10 V bias.

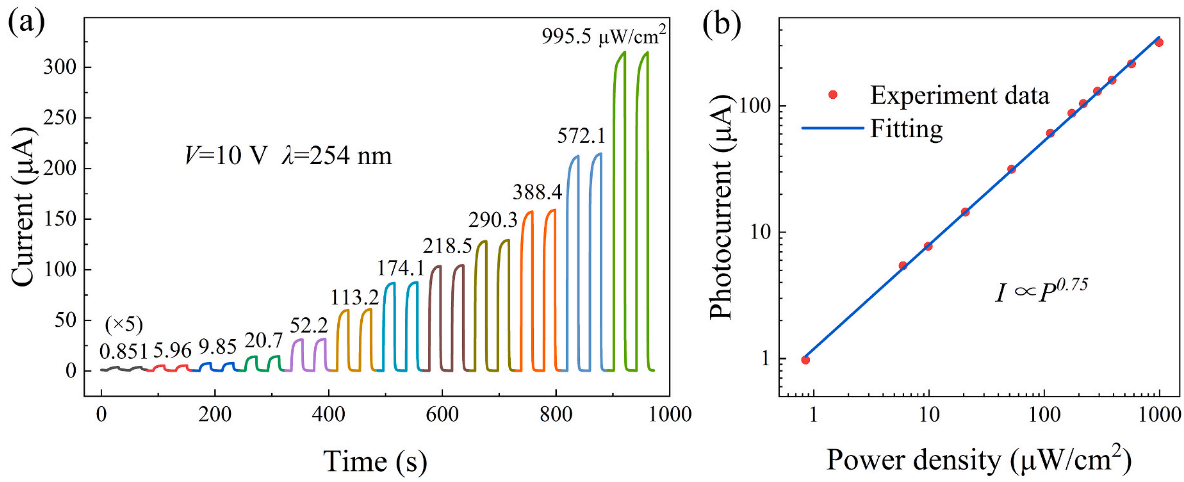

Fig. 5. (a) Time dependence of photocurrent characteristics of the device under various intensity 254 nm light illumination. (b) The photocurrent as the function of various illumination intensities in logarithmic form under 254 nm light biased at 10 V.

time, Fig. 2e displays the cross-sectional SEM image of the device, and we can see that both β-Ga_2O_3 and α-Ga_2O_3 films have the thickness of approximately 100 nm and ITO interdigital electrodes are approximately 150 nm thick. Therefore, the photosensitive area of our device should be the β-Ga_2O_3 film between two ITO electrodes, while α-Ga_2O_3 film on ITO has almost no contribution to photoresponse.

Fig. 3a presents optical transmission spectrum of β-Ga_2O_3 thin film on sapphire substrate, which shows a high transmittance (higher than 90%) in the spectral range of 400–700 nm. And a sharp absorption edge can be obtained at ~250 nm, corresponding to a ~4.9 eV bandgap (the inset of Fig. 3a). In addition, the transmittance of both ITO and α-Ga_2O_3/ITO films was more than 85% throughout the visible band as shown in Fig. 3b, which can meet the requirement of applications with high transparency. Furthermore, the actual photograph of the device (the inset of Fig. 3b) also confirms that it is almost fully transparent to the naked eyes and is very suitable for transparent electronics applications.

Fig. 4a shows the semi-logarithmic *I–V* characteristic curves of transparent Ga_2O_3 UV photodetector in dark and under UV (254 and 365 nm) light (Power density: ~0.6 mW/cm^2) as shown in Fig. 4a. The transparent photodetector shows an ultra-low dark current (1.6 pA@10 V), suggesting the photodetector can be used for the detection of very weak light signals. The normalized photocurrent-to-dark current ratio (NPDR) is a objective metric for evaluating sensitivity of photodetectors, which can avoid the effect of input light intensities. And it can be calculated using the following formula [36,37].

$$NPDR = \frac{I_{photo}/I_{dark}}{P_{\lambda}S}$$

where the parameters include I_{photo} (photocurrent), I_{dark} (dark current), S (effective illumination area of devices) and P_{λ} (power density of light). The calculated NPDR of our device is as high as 4.71×10^{13} W^{-1} under 254 nm light, indicating the excellent solar-blind UV photodetection performance. It is worth mentioning that our photodetector has an ultra-weak photoresponse to the 365 nm illumination, which indicates it has good suppression of the photoresponse from bands over solar-blind UV range. Fig. 4b shows the *I-t* curve of our device irradiated with 254 nm illumination at 10 V. The photodetector exhibits the fast response (~1.63 s of 10–90% rise time; ~0.38 s of 90–10% decay time) to UV light with excellent repeatability and stability.

Fig. 4c shows spectral response curve of the photodetector on a semilogarithmic scale from 200 to 800 nm under 10 V. The maximum responsivity of the device appears at around 250 nm, reaching ~74.9 A/W. Meanwhile, the sharp −3 dB cutoff wavelength can be observed at ~260 nm, indicating a true solar blindness. Typically, UV-to-visible rejection ratio (R_{peak}/R_{400}) is the critical merits to analyze spectral selectivity of photodetector. It can be seen that the rejection ratio of our transparent Ga_2O_3 UV photodetector is 1.3×10^6, suggesting the high spectral selectivity of our device.

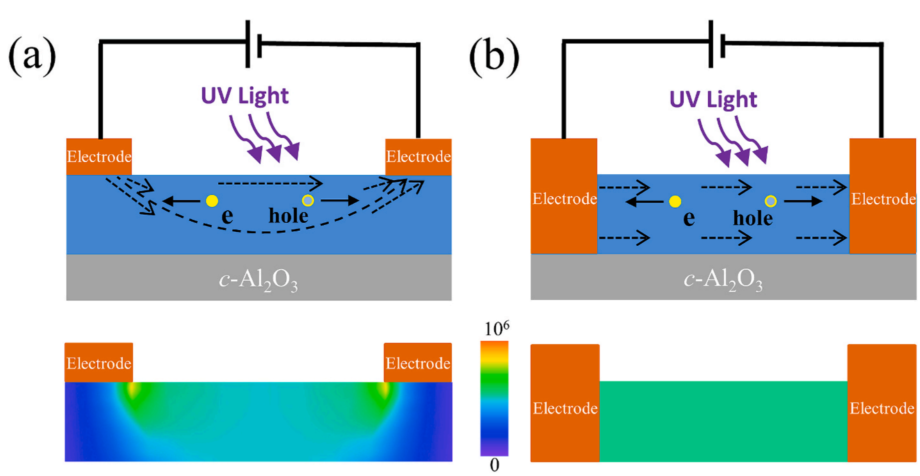

Fig. 6. Schematic diagrams and simulations of electric field distributions for Ga_2O_3 photodetectors with (a) planar structure and (b) embedded structure electrodes under 254 nm UV light illumination.

Table 1
Performance comparison of our transparent device and recently reported typical MSM transparent photodetectors based on Ga_2O_3 thin film.

Materials	Electrode structure	Dark current (nA)	Responsivity (A/W)	Rejection ratio	Detectivity (Jones)	Ref.
α-Ga_2O_3	Planar IZO	~1@200 V	3.2×10^{-4}@10 V	–	2.8×10^{10}	[42]
α-Ga_2O_3	Planar AZO	2.84×10^{-3}@10 V	2.66@10 V	2.93×10^5@10 V (R_{254}/R_{400})	4.84×10^{14}	[43]
α-Ga_2O_3	Planar IZO	11@5 V	43.99@2 V	714.2@2V (R_{250}/R_{555})	–	[31]
α-Ga_2O_3	Planar ITO	–	0.19@20 V	–	–	[44]
β-Ga_2O_3	Planar ITO	3.8×10^{-3}@20 V	181.03@20 V	1.2×10^5@20 V (R_{254}/R_{365})	1.2×10^{15}	[21]
β-Ga_2O_3	Planar ITO	6×10^{-4}@10 V	–	6.83×10^3 (R_{250}/R_{400})	–	[45]
β-Ga_2O_3	Embedded ITO	1.6×10^{-3}@10 V	74.9@10 V	1.3×10^6@10 V (R_{250}/R_{400})	7.4×10^{15}	This work

Fig. 5a displays *I-t* photoresponse curves of our transparent Ga_2O_3 photodetector under 254 nm UV illumination of various intensities at 10 V. With the light density increasing (0.851–995.5 μW/cm^2), currents of device under light irradiation increase obviously with good stability and repeatability. In general, photocurrent (I_{photo}) versus power density (P) are fitted using following simple equation [38,39].

$$I_{photo} = AP^{\theta}$$

where A is a constant and θ is a exponent related to the trap states of the photodetector. As shown in Fig. 5b, θ value was estimated to be ~0.75 by fitting the data which is smaller than 1 (ideal trap-free device), suggesting the existence of the trap states in the Ga_2O_3 photodetector.

The specific detectivity (D^*) is also an critical merit to evaluate UV light detection ability of photodetectors, which is obtained from the following formula [40,41].

$$D^* = \frac{R}{\sqrt{2qI_{dark}/S}}$$

where R, q, I_{dark} and S correspond to the responsivity, the elemental charge, the dark current and the effective illumination area of devices, respectively. Obviously, the calculated D^* value of the photodetector is 7.4×10^{15} Jones, which benefits from its large responsivity and ultra-low dark current.

In order to investigate the reason for the excellent performance of our device, the simulations of electrical field intensity distributions for Ga_2O_3 photodetectors with planar and embedded electrodes were performed by the finite element method as shown in Fig. 6. Under 254 nm UV light illumination, the photogenerated carriers (electron-hole pairs) will be generated in photosensitive layer, which can be separated and moved towards to the electrodes by an applied electric field. It is obvious that for the device with planar electrode structure, the electric field density is greater in the region near the edges of electrodes, but smaller in the region between and under the electrodes. Conversely, when the electrodes are embedded in the β-Ga_2O_3 thin film, a more homogeneous and relatively stronger parallel electric field would be formed inside of the photosensitive layer, which is conducive to the separation and collection of photogenerated carriers. Therefore, the high performance of our transparent photodetector mainly comes from the embedded electrode structure. At the same time, the relatively high crystalline quality of β-Ga_2O_3 photosensitive layer and the device preparation process without etching are also very important factors.

Table 1 presents main performances of our device and some reported typical Ga_2O_3-based transparent photodetectors. Obviously, our device has a UV-to-visible rejection ratio (R_{peak}/R_{400}) of 1.3×10^6 and a specific detectivity of 7.4×10^{15} Jones, which are obviously larger than the recently reported Ga_2O_3-based transparent photodetectors. Additionally, the low dark current or peak responsivity of our transparent photodetector are very competitive or slightly better than the previously reported transparent Ga_2O_3 devices.

4. Conclusions

In summary, a high-performance fully transparent MSM structure solar-blind UV photodetector with embedded ITO electrodes was constructed on Ga_2O_3 film by a novel method without any etching process. That is, the β-Ga_2O_3 film was directly and selectively grown on sapphire substrate with ITO interdigital electrodes prepared in advance. The photodetector exhibits an ultra-low dark current (1.6 pA), a high NPDR (4.71×10^{13} W^{-1}), a large responsivity (74.9 A/W), a superb rejection ratio (1.3×10^6) and a high specific detectivity (7.4×10^{15} Jones) at 10 V. In addition, the estimated rise and decay times are ~1.63 s and ~0.38 s, respectively. The comprehensive performance of our device is superior to previously reported transparent UV photodetectors based on Ga_2O_3 thin films, which can be attributed to its embedded electrode structure and high crystalline quality β-Ga_2O_3. Our work can provide a new method for the fabrication of fully transparent high-performance Ga_2O_3 solar-blind UV photodetectors.

Credit author statement

Chao Zhang: Investigation, Methodology, Formal analysis, Original draft preparation. Kewei Liu: Conceptualization, Validation, Formal analysis, Writing-Review & Editing, Supervision, Resources, Funding acquisition. Qiu Ai: Formal analysis, Resources, Supervision. Xuan Sun: Experimentation supporting. Xing Chen: Resources, Data curation. Jia-lin Yang: Resources, Data curation. Yongxue Zhu: Resources, Data curation. Zhen Cheng: Resources, Data curation. Binghui Li: Resources, Data curation. Lei Liu: Resources, Data curation. Dezhen Shen: Funding acquisition, Supervision, Resources.

Declaration of competing interest

The authors declare that they have no known competing financial interests or personal relationships that could have appeared to influence the work reported in this paper.

Data availability

Data will be made available on request.

Acknowledgements

This work is supported by the National Natural Science Foundation of China (Nos. 62074148, 61875194, 11727902), the National Ten Thousand Talent Program for Young Top-notch Talents, the Key Research and Development Program of Changchun City (No. 21ZY05), Youth Innovation Promotion Association, CAS (No. 2020225), Jilin Province Science Fund (20220101053JC, 20210101145JC), Jilin Province Young and Middle-Aged Science and Technology Innovation Leaders and Team Project (20220508153RC).

References

[1] K. Liu, M. Sakurai, M. Aono, ZnO-based ultraviolet photodetectors, Sensors 10 (2010) 8604–8634.
[2] J. Yang, K. Liu, X. Chen, D. Shen, Recent advances in optoelectronic and microelectronic devices based on ultrawide-bandgap semiconductors, Prog. Quant. Electron. 83 (2022) 100397–100425.
[3] C. Xie, X. Lu, X. Tong, Z. Zhang, F. Liang, L. Liang, L. Luo, Y. Wu, Recent progress in solar-blind deep-ultraviolet photodetectors based on inorganic ultrawide bandgap semiconductors, Adv. Funct. Mater. 29 (2019) 1806006–1806045.

[4] B. Zhao, F. Wang, H. Chen, L. Zheng, L. Su, D. Zhao, X. Fang, An ultrahigh responsivity (9.7 mA W^{-1}) self-powered solar-blind photodetector based on individual ZnO-Ga_2O_3 heterostructures, Adv. Funct. Mater. 27 (2017) 1700264–1700271.

[5] D. Guo, Q. Guo, Z. Chen, Z. Wu, P. Li, W. Tang, Review of Ga_2O_3-based optoelectronic devices, Mater. Today Phys. 11 (2019) 100157–100175.

[6] Q. Cai, H. You, H. Guo, J. Wang, B. Liu, Z. Xie, D. Chen, H. Lu, Y. Zheng, R. Zhang, Progress on AlGaN-based solar-blind ultraviolet photodetectors and focal plane arrays, Light Sci. Appl. 10 (2021) 94–124.

[7] M. Fan, K. Liu, X. Chen, X. Wang, Z. Zhang, B. Li, D. Shen, Mechanism of excellent photoelectric characteristics in mixed-phase ZnMgO ultraviolet photodetectors with single cutoff wavelength, ACS Appl. Mater. Interfaces 7 (2015) 20600–20606.

[8] M. Liao, Y. Koide, J. Alvarez, Photovoltaic Schottky ultraviolet detectors fabricated on boron-doped homoepitaxial diamond layer, Appl. Phys. Lett. 88 (2006) 33504–33506.

[9] Y. Cheng, J. Ye, L. Lai, S. Fang, D. Guo, Ambipolarity regulation of deep-UV photocurrent by controlling crystalline phases in Ga_2O_3 nanostructure for switchable logic applications, Adv. Electron. Mater. (2023) 2201216–2201224.

[10] L. Wang, K. Liu, X. Chen, Y. Zhu, Q. Hou, D. Shen, Fabrication and characteristics of MgZnO ultraviolet detector based on Ag microporous array structure electrode, Chin. J. Lumin. 42 (2021) 201–207.

[11] T. Zhang, M. Li, J. Chen, Y. Wang, L. Miao, Y. Lu, Y. He, Multi-component ZnO alloys: bandgap engineering, hetero-structures, and optoelectronic devices, Mater. Sci. Eng. R. 147 (2022) 100661–100694.

[12] C. Wu, F. Wu, C. Ma, S. Li, A. Liu, X. Yang, Y. Chen, J. Wang, D. Guo, A general strategy to ultrasensitive Ga_2O_3 based self-powered solar-blind photodetectors, Mater. Today Phys. 23 (2022) 100643–100649.

[13] Y. Zhu, D. Zhang, W. Zheng, F. Huang, Multistep thermodynamics yielding deep ultraviolet transparent conductive Ga_2O_3 films, J. Mater. Chem. C 124 (2020) 16722–16727.

[14] D. Kaur, M. Kumar, A strategic review on gallium oxide based deep-ultraviolet photodetectors: recent progress and future prospects, Adv. Opt. Mater. 9 (2021) 2002160–2002193.

[15] J. Xu, W. Zheng, F. Huang, Gallium oxide solar-blind ultraviolet photodetectors: a review, J. Mater. Chem. C 7 (2019) 8753–8770.

[16] C. Wu, L. Qiu, S. Li, D. Guo, P. Li, S. Wang, P. Du, Z. Chen, A. Liu, X. Wang, H. Wu, F. Wu, W. Tang, High sensitive and stable self-powered solar-blind photodetector based on solution-processed all inorganic $CuMO_2/Ga_2O_3$ pn heterojunction, Mater. Today Phys. 17 (2021) 100335–100342.

[17] X. Chen, F. Ren, S. Gu, J. Ye, Review of gallium-oxide-based solar-blind ultraviolet photodetectors, Photon. Res. 7 (2019) 381–415.

[18] C. Wu, F. Wu, H. Hu, C. Ma, J. Ye, S. Wang, H. Wu, J. Wang, A. Liu, D. Guo, Work function tunable laser induced graphene electrodes for Schottky type solar-blind photodetectors, Appl. Phys. Lett. 120 (2022) 101102–101106.

[19] C. Zhang, K. Liu, Q. Ai, X. Huang, X. Chen, Y. Zhu, J. Yang, Z. Cheng, B. Li, L. Liu, D. Shen, Performance enhancement of Ga_2O_3 solar-blind UV photodetector by the combination of oxygen annealing and plasma treatment, J. Phys. Chem. C 126 (2022) 21839–21846.

[20] L.X. Qian, Z. Gu, X. Huang, H. Liu, Y. Lv, Z. Feng, W. Zhang, Comprehensively improved performance of β-Ga_2O_3 solar-blind photodetector enabled by a homojunction with unique passivation mechanisms, ACS Appl. Mater. Interfaces 13 (2021) 40837–40846.

[21] Z. Li, Y. Xu, Y. Cheng, J. Zhang, D. Chen, D. Yao, Q. Feng, S. Xu, J. Zhang, C. Zhang, Y. Hao, Low-temperature processed high-performance visible–transparent Ga_2O_3 solar blind ultraviolet photodetectors with the indium–tin–oxide electrode, Semicond. Sci. Technol. 35 (2020) 125031–125038.

[22] C. Zhou, K. Liu, X. Chen, J. Feng, J. Yang, Z. Zhang, L. Liu, Y. Xia, D. Shen, Performance improvement of amorphous Ga_2O_3 ultraviolet photodetector by annealing under oxygen atmosphere, J. Alloy. Compd. 840 (2020) 155585–155591.

[23] B. Qiao, Z. Zhang, X. Xie, B. Li, K. Li, X. Chen, H. Zhao, K. Liu, L. Liu, D. Shen, Avalanche gain in metal–semiconductor–metal Ga_2O_3 solar-blind photodiodes, J. Phys. Chem. C 123 (2019) 18516–18520.

[24] S. Kee, N. Kim, B. Park, B.S. Kim, S. Hong, J.H. Lee, S. Jeong, A. Kim, S.Y. Jang, K. Lee, Highly deformable and see-through polymer light-emitting diodes with all-conducting-polymer electrodes, Adv. Mater. 30 (2018) 1703437–1703443.

[25] P.-K. Yang, W.-Y. Chang, P.-Y. Teng, S.-F. Jeng, S.-J. Lin, P.-W. Chiu, J.-H. He, Fully transparent resistive memory employing graphene electrodes for eliminating undesired surface effects, Proc. IEEE 101 (2013) 1732–1739.

[26] D. Chen, Z. Liu, B. Liang, X. Wang, G. Shen, Transparent metal oxide nanowire transistors, Nanoscale 4 (2012) 3001–3012.

[27] L. Wang, X. Hu, Transparent electrodes for energy storage devices, Batter. Supercaps. 3 (2020) 1275–1286.

[28] S.-H.K. Park, C.-S. Hwang, M. Ryu, S. Yang, C. Byun, J. Shin, J.-I. Lee, K. Lee, M. S. Oh, S. Im, Transparent and photo-stable ZnO thin-film transistors to drive an active matrix organic-light-emitting-diode display panel, Adv. Mater. 21 (2009) 678–682.

[29] S. Oukassi, L. Baggetto, C. Dubarry, L. Le Van-Jodin, S. Poncet, R. Salot, Transparent thin film solid-state lithium ion batteries, ACS Appl. Mater. Interfaces 11 (2019) 683–690.

[30] L. Wu, H. Fang, C. Zheng, Q. Wang, H. Wang, A multifunctional smart window: detecting ultraviolet radiation and regulating the spectrum automatically, J. Mater. Chem. C 7 (2019) 10446–10453.

[31] N. Kumar, K. Arora, M. Kumar, High performance, flexible and room temperature grown amorphous Ga_2O_3 solar-blind photodetector with amorphous indium-zinc-oxide transparent conducting electrodes, J. Phys. D Appl. Phys. 52 (2019) 335103–335111.

[32] S. Oh, C.-K. Kim, J. Kim, High responsivity β-Ga_2O_3 metal–semiconductor–metal solar-blind photodetectors with ultraviolet transparent graphene electrodes, ACS Photonics 5 (2017) 1123–1128.

[33] H. Wu, Y. Huang, Y. Zhi, X. Wang, X. Chu, Z. Chen, P. Li, Z. Wu, W. Tang, Single-layer graphene electrode enhanced sensitivity and response speed of β-Ga_2O_3 solar-blind photodetector, Opt. Mater. Express 9 (2019) 1394–1403.

[34] K. Liu, B. Dai, V. Ralchenko, Y. Xia, B. Quan, J. Zhao, G. Shu, M. Sun, G. Gao, L. Yang, P. Lei, J. Han, J. Zhu, Single crystal diamond UV detector with a groove-shaped electrode structure and enhanced sensitivity, Sens. Actuators, A 259 (2017) 121–126.

[35] J. Forneris, A. Lo Giudice, P. Olivero, F. Picollo, A. Re, M. Marinelli, F. Pompili, C. Verona, G. Verona Rinati, M. Benetti, D. Cannata, F. Di Pietrantonio, A 3-dimensional interdigitated electrode geometry for the enhancement of charge collection efficiency in diamond detectors, Europhys. Lett. 108 (2014) 18001–18006.

[36] J. Yu, J. Lou, Z. Wang, S. Ji, J. Chen, M. Yu, B. Peng, Y. Hu, L. Yuan, Y. Zhang, R. Jia, Surface modification of β-Ga_2O_3 layer using pt nanoparticles for improved deep UV photodetector performance, J. Alloy. Compd. 872 (2022) 159508–159516.

[37] X. Wang, Z. Cheng, K. Xu, H.K. Tsang, J.-B. Xu, High-responsivity graphene/silicon-heterostructure waveguide photodetectors, Nat. Photonics 7 (2013) 888–891.

[38] D. Han, K. Liu, J. Yang, X. Chen, B. Li, L. Liu, D. Shen, Performance enhancement of a p-Si/n-$ZnGa_2O_4$ heterojunction solar-blind UV photodetector through interface engineering, J. Mater. Chem. C 9 (2021) 10013–10019.

[39] J.M. Choi, H.Y. Jang, A.R. Kim, J.D. Kwon, B. Cho, M.H. Park, Y. Kim, Ultra-flexible and rollable 2D-MoS_2/Si heterojunction-based near-infrared photodetector via direct synthesis, Nanoscale 13 (2021) 672–680.

[40] X. Luo, S. Chen, L. Liu, J. Lv, A. Qadir, K. Shehzad, X. Qiao, Y. Xu, L. Kienle, A. Lotnyk, X. Zhang, G. Qian, X. Fan, Micron-scale photodetectors based on one-dimensional single-crystalline $Sb_{2-x}Sn_xSe_3$ microrods: simultaneously improving responsivity and extending spectral response region, J. Phys. Chem. C 123 (2018) 810–816.

[41] Y. Zhang, X. Chen, Y. Xu, F. Ren, S. Gu, R. Zhang, Y. Zheng, J. Ye, Transition of photoconductive and photovoltaic operation modes in amorphous Ga_2O_3-based solar-blind detectors tuned by oxygen vacancies, Chin. Phys. B 28 (2019) 28501–28506.

[42] W. Tzu-Chiao, T. Dung-Sheng, P. Ravadgar, K. Jr-Jian, T. Meng-Lin, L. Der-Hsien, H. Chiung-Yi, H. Ray-Hua, H. Jr-Hau, See-through Ga_2O_3 solar-blind photodetectors for use in harsh environments, IEEE J. Sel. Top. Quant. Electron. 20 (2014) 112–117.

[43] H. Liu, S. Zhou, H. Zhang, L. Ye, Y. Xiong, P. Yu, W. Li, X. Yang, H. Li, C. Kong, Ultrasensitive fully transparent amorphous Ga_2O_3 solar-blind deep-ultraviolet photodetector for corona discharge detection, J. Phys. D Appl. Phys. 55 (2022) 305104–305112.

[44] S. Cui, Z. Mei, Y. Zhang, H. Liang, X. Du, Room-temperature fabricated amorphous Ga_2O_3 high-response-speed solar-blind photodetector on rigid and flexible substrates, Adv. Opt. Mater. 5 (2017) 1700454–1700462.

[45] Y. Sui, H. Liang, W. Huo, Y. Wang, Z. Mei, A flexible and transparent β-Ga_2O_3 solar-blind ultraviolet photodetector on mica, J. Phys. D Appl. Phys. 53 (2020) 504001–504009.